

Structural and Electrical Properties of Ni-Zn Ferrite Nanoparticles: Influence of Mixed Fuel Approach

V.R. Bhagwat¹, M. N. Sarnaik², V. D. Murumkar³, K. M. Jadhav⁴

Department of Physics, Deogiri College Aurangabad (M.S.) India¹

Muktanand College, Gangapur, Aurangabad (M.S.) India²

Department of Physics, Vivekanand College, Aurangabad (M.S.) India³

Department of Physics, Dr. Babasaheb Ambedkar Marathwada University, Aurangabad, (M.S.) India⁴

Abstract: Ni_{0.5}Zn_{0.5}Fe₂O₄ (Ni-Zn) ferrite nanoparticles were synthesized by sol-gel auto combustion method using mixed fuel approach (citric acid and ethylene glycol) as a fuel. The metal nitrate to fuel ratio was taken as 1:(1:3). The as synthesized powder of Ni-Zn ferrite nanoparticles is annealed at 650 °C for 5 h and prepared sample was used for characterization and investigations of structural and electrical properties. The structural characterization of Ni-Zn ferrite nanoparticles were done by X-ray diffraction technique. The average crystallite size obtained by Scherrer's formula is of the order of 21 nm. The lattice constant determined from XRD data is in the reported range 8.3783 Å. The DC electrical resistivity was investigated from room temperature to 850 K using two probe techniques. DC electrical resistivity behaviour of Ni-Zn ferrite nanoparticles suggests that the sample is semiconducting in nature.

Keywords: Ni-Zn ferrite; sol-gel auto combustion; XRD; citric acid and ethylene glycol.

I. INTRODUCTION

Ferrites are ferrimagnetic oxides consisting of ferric oxide and metal oxides. On the basis of crystal structure ferrites are grouped into three classes namely garnet, spinel and hexagonal ferrite. The spinel ferrites are widely studied because of their superior properties such as structural, magnetic, electrical and catalytic properties, all of which are different from those of their bulk counterparts and applications point of view in various and new fields like magnetic drug delivery, catalyst, sensors, biological, biomedical and medical science [1-4]. The spinel ferrite has the general formula of M-Fe₂O₄ where M is a divalent metal ion (Mn, Co, Ni, and Zn etc). Among spinel ferrites, Ni-Zn ferrite (CoFe₂O₄) has an inverse spinel structure and promising magnetic material for high-density recording applications because of their high magneto crystalline anisotropy, high coercivity, moderate saturation magnetization and high chemical and structural stability at higher temperatures, which make it a good candidate for the electronic components used in computers, recording devices, and magnetic cards [5-9]. The properties of nanoparticles mostly depend on synthesis method therefore nowadays different synthesis methods are being used for synthesis nanomaterials. Ni-Zn ferrite nanoparticles have been synthesized using various methods, such as co-precipitation method, hydrothermal method, micro emulsion method, sol-gel method, sonochemical reaction method, ball milling, laser ablation and aerosol method [10-14]. Among synthesis methods, sol-gel auto combustion method has been used for synthesis of Ni-Zn ferrite nanoparticles. Auto-combustion

synthesis process is based upon the thermo-chemical concept used in the field of propellants and explosives, its extrapolation to the combustion synthesis of nano-oxides. A various fuels have been used in the combustion synthesis of ferrite nonmaterial, like glycine, urea, oxalyl-hydrazine, citric acid, and sucrose. All these fuels serve two purposes: (i) they are the source of C and H, the reducing elements, which form CO₂ and H₂O on combustion and liberate heat; and (ii) they form complexes with the metal ions facilitating homogeneous mixing of the cations in solution. The exothermicity of the redox reaction ranges from 1200 K to 1800 K. The nature of combustion differs from flaming to non-flaming depending upon which fuel used for preparation of nano-material. In the present work new approach has been used to prepare Ni-Zn ferrite nanoparticles using mixed fuel (citric acid and ethylene glycol). To date very less work have been reported using mixture of citric acid and ethylene glycol.

The present research reports deals with the synthesize Ni-Zn ferrite nanoparticles by sol-gel auto combustion method using mixture of citric acid and ethylene glycol as fuel and to investigate the structural and magnetic properties of Ni-Zn ferrite nanoparticles. In the literature, structural and magnetic properties of Ni-Zn ferrite nanoparticles are reported, but no systematic investigation of their electrical behaviour is reported. The electrical properties of spinel ferrite nanoparticles are important from the point of view of its use in transformer cores, humidity and gas sensor devices.

II. EXPERIMENTAL

The Ni-Zn nanoparticles were synthesized by sol-gel auto-combustion method using citric acid + ethylene glycol as a fuel. The metal nitrates to fuel ratio was taken as 1: (1:3) or (metal nitrate: (citric acid: ethylene glycol). All the reagents used for the synthesis of Ni-Zn ferrite nanoparticles were analytical grade and used as received without further purification. The stoichiometric proportion of nickel nitrate $Ni(NO_3)_2 \cdot 6H_2O$, zinc nitrate $Zn(NO_3)_2 \cdot 6H_2O$, ferric nitrate $Fe(NO_3)_3 \cdot 9H_2O$, citric acid $C_6H_8O_7 \cdot H_2O$ and ethylene glycol $C_2H_6O_12$ were separately dissolved in minimum amount of distilled water using magnetic stirrer. After complete dissolution of metal nitrates in distilled water then Ni-Zn nitrate and ferric nitrate solution were mixed and stirred sometime with constant heating at $90^\circ C$. After some stirring mixed citric acid + ethylene glycol solution was added to the nitrates solution. The all solution was again stirred for about 6 h at 90° Con a hot plate with continuous stirring until it becomes viscous and finally formed a very viscous gel. The temperature is further raised up to $120^\circ C$ so that the ignition of the gel suddenly starts. The dried gel was subsequently swelling into foam like and undergoes a strong self-propagating combustion reaction to give a loose Ni-Zn ferrite nano-powder. Finally the as prepared loose $Ni_{0.5}Zn_{0.5}Fe_2O_4$ ferrite powder was grinded for 30 min and annealed at $650^\circ C$ temperature for 5 h in muffle furnace to improve the ordering and for further characterization.

Characterizations

The crystalline phase of the prepared $Ni_{0.5}Zn_{0.5}Fe_2O_4$ ferrite sample was identified by X-ray diffraction technique using XPERT-PRO system. X-ray powder diffractions were performed at room temperature using monochromatic Cu- K_α radiation with $\lambda=1.54060 \text{ \AA}$ operated at 40 kV and 35 mA with 2θ ranging from 20° to 80° at a step size 0.02° per second. DC electrical resistivity was measured by two probe method. A small constant voltage was applied across the sample and the current through the sample was measured with respect to temperature. Temperature of the sample in the form of pellet was measured with chromel-alumel thermocouple.

III. RESULTS AND DISCUSSIONS

Fig. 1 shows the XRD pattern of the annealed $Ni_{0.5}Zn_{0.5}Fe_2O_4$ ferrite nanoparticles. The diffraction peaks observed at $2\theta= 30.32^\circ, 35.65^\circ, 43.33^\circ, 53.67^\circ, 57.24^\circ, 62.80^\circ$ corresponding to the (220), (311), (400), (422), (511) and (440) planes, respectively. In this XRD pattern other oxides or impurity phases are not detected therefore XRD patterns confirm the formation of cubic spinel type lattice of $CoFe_2O_4$, which matches well with the standard XRD pattern (JCPDS No: 22-1086). The lattice constant (a) of Ni-Zn ferrite samples was obtained from the following equation.

$$a = d\sqrt{(h^2+k^2+l^2)} \quad \text{\AA} \quad (1)$$

where, (h k l) are the Miller Indices, d is inter planner spacing. Thus, lattice constant was computed using the d value and the (h k l) parameters.

The crystallite size (D) has been calculated from FWHM (full width at half maximum) of most intense peak (311) data using Debye-Scherrer's equation [15].

$$D = \frac{(0.9 \lambda)}{(\beta \cos \theta)} \quad \text{nm} \quad (2)$$

where, D is the crystallite size, λ is the wavelength of Cu- K_α (1.5405 \AA), β is the full width at half maxima of the most intense diffraction peaks and θ is the Bragg's angle. The reflection from (311) plane was used for determination of average crystallite size.

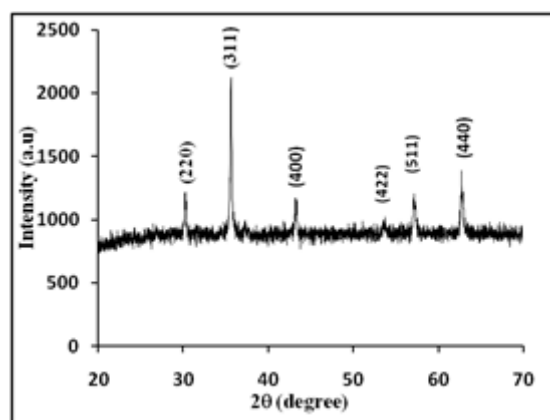


Fig. 1. XRD pattern of Ni-Zn ferrite nanoparticles

The unit cell volume (V) was calculated by using the following equation;

$$V = a^3 \quad [A] \quad (3)$$

where, V is the volume of unit cell, 'a' is the lattice constant.

The X-ray density (ρ_b) of the sample was calculated using the relation [16].

$$\rho_b = \frac{8M}{N_A a^3} \quad \text{gm/cm}^3 \quad (4)$$

Where, M is the molecular weight and N_A is the Avogadro's number and 'a' is the lattice parameter. As there are 8 molecules in the unit cell, so 8 is included in the formula. The bulk density (ρ_m) of Ni-Zn ferrite sample was determined using standard formula.

$$\rho_m = \frac{m}{\pi r^2 t} \quad \text{gm/cm}^3 \quad (5)$$

Where, m is mass of pellets, r is the radius of pellets and t is thickness of pellet.

The structural parameters such as lattice constant, unit cell volume, X-ray density, bulk density and specific surface area of Ni-Zn ferrite nanoparticles are given in Table 1. From table 1, it was understood that the calculated values of lattice constant of Ni-Zn ferrite nanoparticles is 8.378 \AA which agree with the reported values [17]. The crystallite size of the Ni-Zn ferrite nanoparticles is 16 nm. Small crystallite size is due to using mixed. The X-ray density is found to be of the order of 5.301 gm/cm^3 . The

bulk density of Ni-Zn ferrite nanoparticles was measured from the standard formula [18].

TABLE I Lattice constant, volume of unit cell, X-ray density, bulk density and average crystallite size from XRD data

| Structural Parameters | Values |
|----------------------------|-------------------------|
| Lattice constant (a) | 8.379 Å |
| Volume of unit cell (V) | 588.0 Å ³ |
| X-Ray density (ρ_x) | 5.302 g/cm ³ |
| Bulk density (ρ_b) | 2.749 g/cm ³ |
| Crystallite size (t) | 21.23 nm |

The value of bulk density is of the order of 2.749 gm/cm³. It was observed that X-ray density of sample is greater than its bulk density. This was due to the pores present in the prepared materials. The increase in porosity is due to preparation condition [19]. All the structural data of prepared Ni-Zn ferrite nanoparticles is in the reported range.

Electrical Properties

The electrical behavior of Ni-Zn ferrite nanoparticles was studied by measuring dc resistivity as a function of temperature using two probe techniques. Temperature variation of dc resistivity is shown in Fig. 2 It is evident from Fig. 2 that the plot of log ρ versus $1000/T$ exhibit the similar nature to that of bulk Ni-Zn ferrite. It can be further observed from Fig.2 that resistivity decreases with increase in temperature indicating the semiconducting nature of the samples and obeys the Arrhenius relation [20];

$$\rho = \rho_0 e^{(\Delta E/kT)} \quad (6)$$

where, ρ_0 is resistivity at room temperature, k is the Boltzmann constant, ΔE is the activation energy and T is the absolute temperature.

The resistivity plot shows two regions high temperature region (ferrimagnetic) and low temperature region (paramagnetic) separated at a particular temperature which may correspond to Curie temperature of Ni-Zn ferrite. A change in slope is contributed to change in conduction mechanism or phase transition from ferrimagnetic to paramagnetic. The conduction mechanism can be explained on the basis of Verwey model [21].

According to Verwey, the conduction mechanism in ferrite occurs mainly due to hopping of Fe²⁺ and Fe³⁺ ions in the octahedral [B] site. It is well known that hopping probability depends upon the separation between ions and the activation energy. The activation energy can be determined from slope of the linear plots of dc electrical resistivity (Fig. 2) and the Arrhenius relation [Eq.8]. The calculated value of activation energy is of the order of 0.397eV. The activation energy of material is associated with mobility of charge carrier. The charge carriers are located with ions or vacant site and conduction takes place through hopping process.

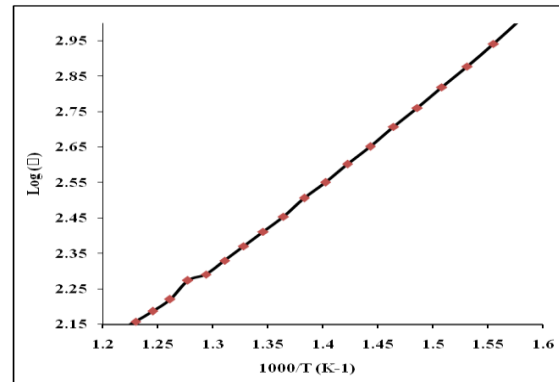


Fig.2. Temperature dependence of dc resistivity of Ni-Zn ferrite nanoparticles

IV. CONCLUSION

Ni_{0.5}Zn_{0.5}Fe₂O₄ ferrite nanoparticles have been synthesized successfully by sol-gel auto combustion method using mixed fuel. X-ray diffraction pattern confirms the formation of cubic spinel structure in single phase without any impurity peak. The average crystallite size is obtained was of the order 21 nm. The lattice constant and other structural parameter are in the reported range. The D.C. electrical resistivity decreases with increase in temperature obeying Arrhenius plot. The activation energy calculated from D.C electrical resistivity versus temperature is of the order of 0.397 eV.

REFERENCES

- [1] V. J. Sawant, S. R. Bamane, Int. J. Pharm. Sci. Rev. Res. 20 (2013) 159.
- [2] M. Kooti, M. Afshari, ScientiaIranica. 19 (2012) 1991.
- [3] J. A. Paulsen, A. P. Ring, and C. C. H. L, J. of Applied Physics 97 (2005) 044502.
- [4] O. Caltun, G.S.N. Rao, K.H. Rao, J. of Magn. and Magnetic Materials 00 (2006)
- [5] S. Amiri, S. shokrollahi. Material Science and Engineering C 33(1) (2013)1.
- [6] M. H. Sousa, F. A. Tourinho, J. Depeyrot, G. J. da Silva, and M. C. F. L. Lara, J. Physical Chem. B. 105 (2001) 1168.
- [7] Z. Chen and L. Gao, Mater. Sci. and Eng: B.141 (2007) 82.
- [8] A. P. Alivisatos, Science. 271 (1996) 933.
- [9] M. Sugimoto, J. of the Amer. Ceramic Society. 82 (1999) 269.
- [10] Yue Zhang, Zhi Yang, Di Yin, Yong Liu, J. Magn. and Magnetic Materials 322 (2010) 3470
- [11] A. Cabañas and M. Poliakoff, J. Mater. Chem., 11 (2001) 1408.
- [12] Y. Ahn, E. J. Choi, S. Kim, and H. N. Ok. Mater Letters 50 (2001) 47.
- [13] J.-G. Lee, J. Y. Park, and C. S. Kim, J. Mater. Science 33 (1998) 3965.
- [14] K. V. P. M. Shafi, A. Gedanken, R. Prozorov and J. Balogh, Chem. of Materials, 10 (1998) 103445
- [15] B.D.Cullity, Elements of X-Ray Diffraction, Second ed., Addison-Wesley. (1967).284.
- [16] Khirade, P. P., Birajdar, S. D., Humbe, A. V., & Jadhav, K. M. (2016), Journal of Electronic Materials, 45(6), 3227-3235.
- [17] M. George, S.S. Nair, A.M. John, P. A. Joy, J. Phys. D: Appl. Phys. 39 (2006) 900.
- [18] S. P. Yadav, S. S. Shinde, A. A. Kadam, and K. Y. Rajpure. Journal of Semiconductors. 34 (2013) 093002
- [19] Sagar E. Shirsath, B.G. Toksha and K.M. Jadhav. Mat. Chem. Phys. 117 (2009) 163.
- [20] Khirade, P. P., Birajdar, S. D., Raut, A. V., & Jadhav, K. M. (2016), Journal of Electroceramics, 37(1-4), 110-120.
- [21] R. D Waldron, Physical review. 99 (1955) 1727.